Characteristics of the Rough-Cut Surface of Quenched and Tempered Martensitic Stainless Steel Using Wire Electrical Discharge Machining

C.A. HUANG, G.C. TU, H.T. YAO, and H.H. KUO

This article studies the surface characteristics of quench- and temper-treated AISI 440A martensitic stainless steels, which were rough cut using wire electrical discharge machining (WEDM). The microstructure of the recast layer on the cut surface was investigated using scanning and transmission electron microscopes, and the phase compositions were analyzed with an energy-dispersive X-ray (EDX) spectrometer. Experimental results showed that the thickness of the recast layer varied with the heat-treatment condition of the workpiece, the largest thickness was obtained with a quenched specimen, and the thickness decreased with increasing tempering temperature. Intergranular surface cracks were observed only from the as-quenched specimen, whereas surface cracks were not found in the rough-cut specimens after tempering above 200 °C. It is reckoned that reliefing of the thermal residual stress in the quenched workpiece induced the surface intergranular cracks. Microstructures of the recast layer on the rough-cut surfaces of the 600 °C tempered specimen were examined using cross-sectional transmission electron microscopy (TEM) specimens. An amorphous layer exists at some parts of the outermost cut surface. A high density of wire electrode droplets of spherical shape, approximately 10 to 60 nm in size, was found throughout the porous recast layer. Besides, many high-chromium containing sigma spheres with sizes of approximately 120 to 200 nm were precipitated at the bottom part of the recast layer, and its formation mechanism was proposed. Adjacent to the recast layer was a heat-affected zone (HAZ) with a thickness of about 4 μm, in which temper-induced carbides were fully dissolved. The HAZ comprised basically two distinct regions: the first region adjacent to the recast layer was composed of a lath martensite structure, while the other region was an annealed ferrite structure.

I. INTRODUCTION

MARTENSITIC stainless steels are widely used in plastic injection molds, surgical tools, and mechanical parts, owing to their superior corrosion resistance, high strength, and good wear resistance. In practical usage, these steels are often quenched from 1100 °C to 1200 °C to obtain the martensitic structure, which has the highest strength and hardness because of the saturated solution of carbon and high dislocation density in the matrix. Due to the low toughness of the martensitic structure, a temper treatment between 200 °C and 650 °C after quenching is needed to obtain suitable mechanical properties. With increasing temper temperatures, carbides such as $M_{23}C_6$, M_7C_3, and M_3C precipitate[1] in the matrix, inducing a tempered martensitic structure with multiple phases[2] and enhancing the toughness of material. In general, martensitic stainless steels are quenched and then tempered before shape cutting using wire electrical discharge machining (WEDM), which is widely used for final surface finishing of hardened mold materials.

C.A. HUANG, Associate Professor, is with the Department of Mechanical Engineering, Chang Gung University, Taoyuan, Taiwan, Republic of China. Contact e-mail: gfehu@mail.cgu.edu.tw G.C. TU, Professor, is with the National Chiao Tung University, Hsinchun, Taiwan, Republic of China. H.T. YAO, Manager, is with Sun Chain Trading Co., Ltd., Taipei, Taiwan, Republic of China. H.H. KUO, Doctoral Candidate, is with the Department of Materials Science and Engineering, National Taiwan University, Taipei, Republic of China.

Manuscript submitted April 30, 2001.

The WEDM apparatus cuts metal by discharging electrical current across a gap, filled with dielectric fluid, between the workpiece and a continuously moving wire electrode. The generated discrete spark produces a tiny crater *via* melting and even vaporization, thus, eroding the workpiece to produce complex two- and three-dimensional shapes with a computer numerically controlled (CNC) machine. The material-removal mechanism of the WEDM apparatus is the same as that of electrical discharge machining (EDM). It has been accepted that the metal-removal phenomenon with EDM is predominantly a thermal effect in nature.[3] During the electrical discharge, an avalanche of electrons and plasmas strike both the wire electrode and workpiece. This electrical discharge generates an enormous amount of heat, causing local melting or even evaporation of the surfaces of both the wire electrode and the workpiece. The heat also causes boiling of the dielectric fluid and the induced high-pressure impact bombarding the molten or vaporized metal into pieces in all directions, which are then carried away by the newly injected cold dielectric fluid. Therefore, craters are formed on both electrodes with each spark—namely, a large one formed on the workpiece and a smaller one on the wire electrode. Besides the surface defects such as cracks, gas voids, plastic deformation, and the buildup of residual stress caused by the rapid cooling rate at the end of discharging,[4–7] a recast layer is always formed on the electrical-discharged surface, which is composed of several microscopic metallurgical layers, dependent on the machining conditions, electrode materials, and discharge mechanisms.[4,6,8,9]

Although WEDM has been used for many decades, few works have studied the microstructure of the recast and

heat-affected zone (HAZ) of the surface processed by WEDM. This situation is perhaps due to the fact that the recast and HAZ of the surface processed by WEDM is so thin that the behavior is difficult to study. The purpose of this article is to investigate the characteristics of the recast layer after a WEDM rough cut on a quenched and tempered martensitic stainless steel. Moreover, the microstructure of the recast layer and HAZ on a surface processed by WEDM of a 600 °C tempered specimen, which has suitable mechanical properties and is widely used in industry, was fully studied with transmission electron microscopy (TEM).

II. MATERIAL TREATMENT AND EXPERIMENTAL PROCEDURES

The commercial as-rolled martensitic stainless steel (AISI 440A), with the composition given in Table I, was used for the present investigation. Before the WEDM's rough-cutting experiment, all the specimens, with dimensions of 80 × 80 × 15 mm^3, were quenched in water from 1100 °C and tempered for 30 minutes at 200 °C, 400 °C, and 600 °C.

The WEDM rough-cutting experiment was performed with a Charmilles Technologies Robofil 300 five-axis computer numerical control (CNC) machine (Charmilles Technologies S.A. Geneva, Switzerland). A 0.25-mm-diameter brass wire electrode was used. The dielectric fluid used was deionized (DI) water, which has a resistivity of 15×10^6 Ω cm, a temperature of 20 ± 0.5 °C, and a flushing pressure of 550 MPa. All rough-cut operating parameters were selected according to the expert system saved in the WEDM apparatus and are expressed in Table II.

To identify microstructures of the surface processed by WEDM, a PHILIPS* 515 scanning electron microscope and a JEOL* 2010 transmission electron microscope equipped with an energy-dispersive X-ray (EDX) to spectrometer allow for chemical analysis were used. To prepare the scanning electron microscopy (SEM) cut surface, the sample was sectioned perpendicular to the cutting surface and approximately 5 mm from the workpiece surface and then mounted in epoxy resin face to face in the center, to minimize an uneven surface or taper during subsequent grinding and polishing. After mechanically lapping and, finally, polishing the surface with diamond paste to a mirror finish, the specimen was immersed in an etching solution for 3 minutes to reveal the recast-layer structure. The etching solution consisted of 1 g picric acid, 5 mL HCl, and 100 mL methanol. After being rinsed with DI water, dried in cold air, and placed in a vacuum chamber, the samples were then ready for microstructure examination. The thickness of the recast layer was evaluated from the SEM micrographs of the mentioned cross-sectional specimen, on which a set of parallel lines was drawn. The thickness and standard deviation of thickness were calculated based on the sectioned length of recast layers on the SEM pictures, using 500 times magnification. For meaningful statistical evaluation, at least 100 lines were drawn for each specimen.

Cross sectioned specimens for TEM examination were obtained from specimens tempered at 600 °C, which provides suitable mechanical properties (strength, hardness, and toughness) and is widely employed in industry. The same method used to prepare the SEM specimen of the cutting surface was employed to prepare the TEM specimen. The cut surface was sectioned with WEDM to dimensions of 1-mm thick, 1.5-mm long, and 1-mm wide and was then stuck face to face with M-Bond 610 and mounted vertically in a copper ring 3 mm in diameter using G1 epoxy (Gatan Company, Pleaston, CA). The specimen was then mechanically ground to 100 μm in thickness, and the two sides of the specimen were further dimpled with Dimpler (VCR, Dimpler) to a thickness of 10 μm at the center. Finally, a low-angle (~8 deg) Ar^+-ion milling machine (VCR Group Inc., San Francisco, CA, XLA 2000) operated at 5 kV was used to sputter the specimen until a tiny hole was produced in the adhered rough-cut interface, around which the cut surface was so thin that the electron diffraction and image could be observed and examined with the TEM/EDX apparatus. During the ion milling, the specimen holder was chilled with liquid nitrogen to avoid heating the specimen. The preparation procedure has also been described elsewhere.[10,11]

III. RESULTS AND DISCUSSION

A. *The Thickness of the Recast Layer*

Figures 1(a) through (d) show the SEM cross-sectional micrographs of rough-cut specimens, which were quenched and then tempered at 200 °C, 400 °C, and 600 °C. All specimens were etched to reveal the recast layer/substrate interface. Accompanying the etching, substrate grain boundaries approximately 0.8-μm wide were also observed in Figures 1(b) and (c), which are virtually different from the cracks observed on quenched specimens, as will be described later,

*PHILIPS is a trademark of Philips Electronic Instruments Corp., Mahwah, NJ.

*JEOL is a trademark of Japan Electron Optic Ltd., Tokyo.

Table I. Chemical composition of martensitic stainless steel (AISI 440A)

Element	C	Cr	Mo	Mn	Si	S	P	Fe
Wt pct	0.60 to 0.75	16.0 to 18.0	0.75	1.00	1.00	0.03	0.04	remainder

Table II. Operating Parameters of the WEDM Rough-Cutting Experiment

Parameter	Voltage (V)	Current (A)	A (μs)	B (μs)	WS (m/min)	WB (daN)
Value	−80	4	1.0	9.0	10	1.0

A: duration of discharging time; B: time between two pulses; WS: wire feeding speed; and WB: wire tension.

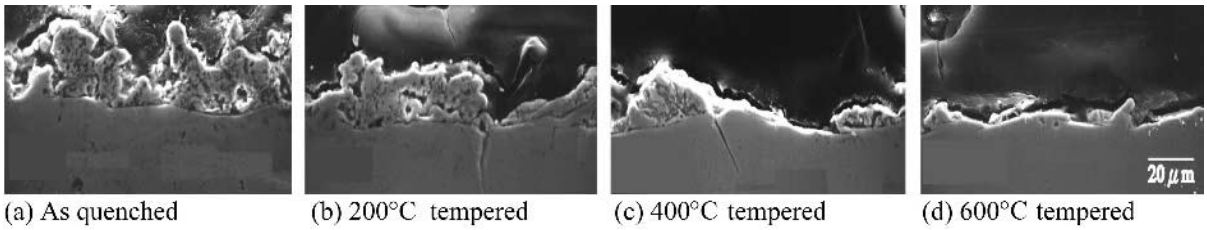

Fig. 1—Recast layers of as-quenched and 200 °C, 400 °C, and 600 °C tempered specimens after WEDM rough cutting (SEM micrograph, specimen etched).

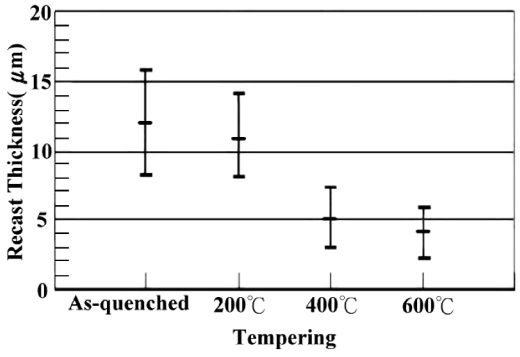

Fig. 2—The thickness and standard deviation of the recast layer for the specimens.

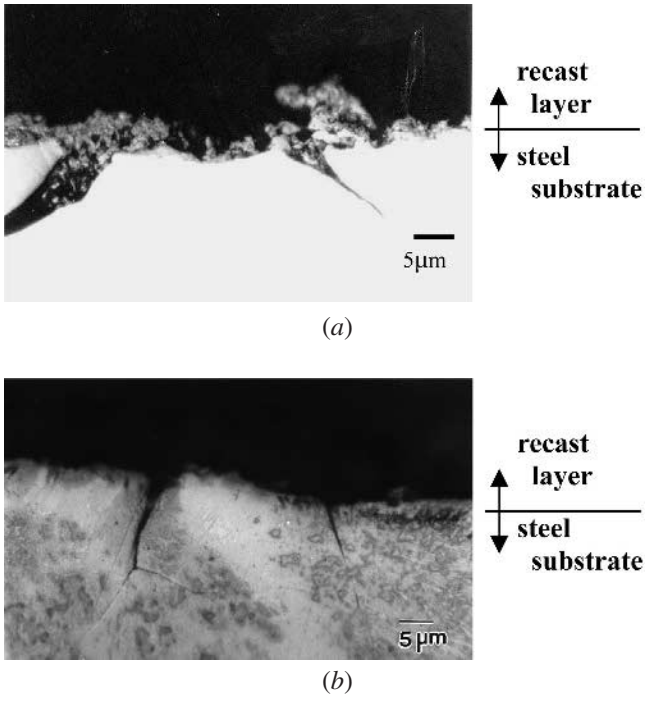

Fig. 3—Cross-sectional examination of quenched specimen after WEDM rough cutting showing (*a*) surface cracking, unetched specimen; and (*b*) intergranular cracking, chemically etched specimen (optical micrograph)

judging from the large differences in the etched boundary and crack widths. It is obvious that the thickness of the recast layer decreases with increasing tempering temperature. The thickness of the recast layer on the quenched specimen was found to be approximately 12-μm thick, but it was reduced to approximately 4-μm thick on the specimen tempered at 600 °C (Figure 2). That is, the thickness of the recast layer varied with the tempering condition of the workpiece: the largest thickness was obtained with the quenched specimen, and the thickness decreased with increasing tempering temperature.

The different thicknesses of the recast layers related to workpiece tempering condition can be explained as follows: the material-removal mechanism, with electrical discharging machining, proposed by Zolotych[12] indicated that the material was first molten or even evaporated through electrical discharging, and the local spot temperature of the discharge can reach as high as 6000 °C.[3,12] Some molten or evaporated material was removed from the injection of the dielectric fluid, and the remaining molten material was cooled down on the cut surface to form a recast layer. During the heating stage of WEDM, the quenched workpiece tends to transform from the martensite to gamma phase, while the tempered workpiece tends to transform from the carbide and ferrite phases to gamma phase. Longer time or more heat for the transformation of the latter are required to dissolve the carbides into the ferrite phases through the diffusion process. This mechanism would also cause a correspondingly less quantity of the liquidized or vaporized workpiece. Therefore, the molten region of the quenched steel after the same heating by electrical discharging is larger than that of the steel tempered at higher temperatures. Since the recast layer is formed from solidification of the molten material and the larger molten region was achieved for the martensite structure by electrical discharging, it possibly resulted in the final thicker recast layer for quenched steel. Some researchers[8,9,13] have proposed that the thickness of the recast layer is affected by the heat conductivity, and, thus, the higher heat conductivity of the material, the smaller the recast thickness. However, in this study, the thickness of the recast layer revealed that the thickness could also be affected by the different heat treatments of the workpiece.

B. *Intergranular Cracking of Surface Processed by WEDM*

As shown in Figures 3(a) and (b), surface intergranular cracking, of approximately 3.5 to 5 μm in width, was observed from the cross-sectional quenched specimen after rough cutting. However, these surface cracks were not found from the specimens tempered above 200 °C. Because of the thermal stress and phase transformation, the residual stress rose severely as the martensitic stainless steel was quenched rapidly from 1100 °C.[2] That is, during quenching, the structure of the steel transformed rapidly from high-temperature stable austenite

(fcc structure) to carbon-oversaturated martensitic phase (bct structure), and the thermal residual stress was also developed. When the plate specimen was rough cut with the wire electrode, the residual stress near the cut surface was released without constraint. The experimental observation confirmed that relief of the quench-induced residual stress on the cut surface was through intergranular surface cracking. To avoid surface cracking after WEDM rough cutting, a lower residual stress is required and a tempering treatment above 200 °C is needed for the steel after quenching.

Figure 4(a) shows that the recast material was found to have filled the inside of a crack of an approximately 16 μm in width, and the EDX analysis of this recast material is shown in Figure 4(b). Comparing with the EDX analysis of the substrate steel (Figure 4(c)), the copper and zinc elements of the wire electrode and the iron and chromium elements of substrate steel were detected. That is, the recast material within the the crack consists of both wire and substrate materials. It is, therefore, suggested that during the WEDM rough cutting, the surface crack must initiate and propagate very quickly along the grain boundary for the crack tip to be filled with the molten material induced by electrical discharging.

It is also interesting to find that, in the EDX analysis on the recast material within the crack, much more chromium was detected within the crack than within the substrate steel (comparing Figures 4(b) and (c)). It is, therefore, suggested that segregation or precipitation of another Cr-rich phase may be induced in the recast layer during solidification. To examine such segregation or precipitation of chromium, cross-sectional TEM specimens were prepared and investigated, as discussed in the following section.

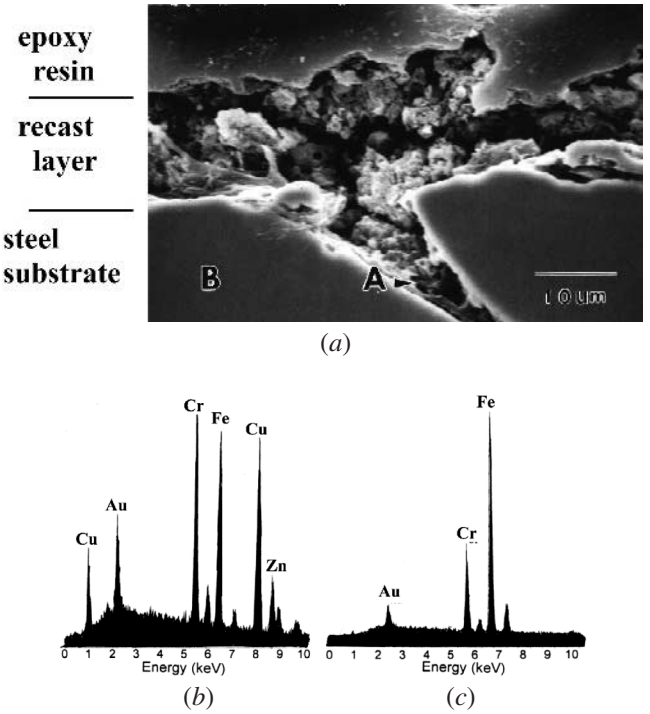

(*a*) (*b*) (*c*)

Fig. 4—(*a*) Intergranular surface crack of quenched specimen after WEDM, within which recast material filled (SEM micrograph, specimen etched). (*b*) EDX analysis of point A arrow indicated in (a). (*c*) EDX analysis of point B of the substrate steel in (a).

C. *Microstructure of the Rough-Cut Surface Processed by WEDM*

A cross-sectional 600 °C tempered specimen of the WEDM rough-cut surface was prepared for TEM examination. As shown in Figure 5(a), an amorphous layer was found on some parts of the outermost cutting surface, which underwent rapid heating by electrical discharging and cooling by the dielectric fluid. Inside the amorphous layer, fine crystalline particles (approximately 10 nm) are randomly distributed. The diffraction pattern of the white circled region containing amorphous and fine crystallites is shown in the right-hand corner of Figure 5(a), in which a broadened ring with a faint background (amorphous) and point-diffraction pattern (nanocrystalline) were detected. It has been proposed by Duwez that the cooling rate must be as high as 10^6 to 10^8 K/s to form metallic glass during solidification or even deposition from the vapor phase.[14] Thus, the solidification rate of this amorphous layer found at the local outermost surface must be very rapid. However, in some parts of the local outermost surface, the amorphous layer was substituted with a microcrystalline layer, as observed in Figure 5(b), and numerous electrode deposits were present in this outermost surface region. The

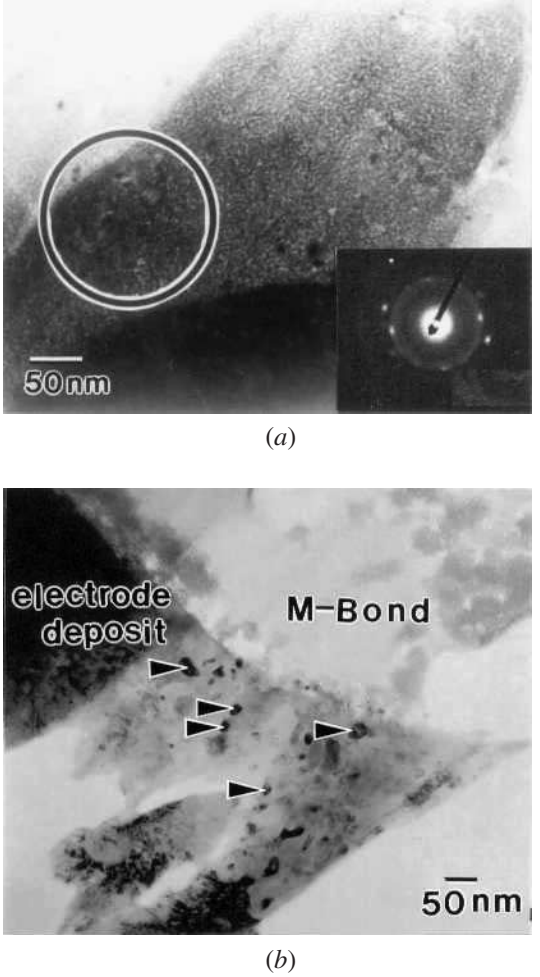

(*a*) (*b*)

Fig. 5—TEM micrographs showing two outermost structures of WEDM rough-cutting surface, specimen tempered at 600 °C: (*a*) amorphous layer at outermost cut surface and its SAD of white-circled area and (*b*) microcrystalline layer at outermost cut surface.

amorphous structure was found from place to place and was distributed randomly on the outermost surface.

Next to the amorphous layer, as seen in the region beneath the amorphous layer (Figure 5(a)), a high density of spherical deposits composed of materials form the wire electrode was found. Bright- and dark-field TEM micrographs, shown in Figure 6, depicted these spherical electrode deposits, and they were also found throughout the recast layer (refer also to Figures 5, 8(a), and 9). Two definite phases were detected inside most of the recast layer, owing to the rapid solidification of the recast material, which contains the materials of the wire electrode and the martensitic stainless steel. The TEM micrograph of Figure 7 shows many wire-electrode deposits at the side of a gas void within the recast layer. The formation of this gas void is caused by gas bubbles, which were formed by evaporated dielectric fluid and were not fully excluded from the molten metal during electrical discharging.

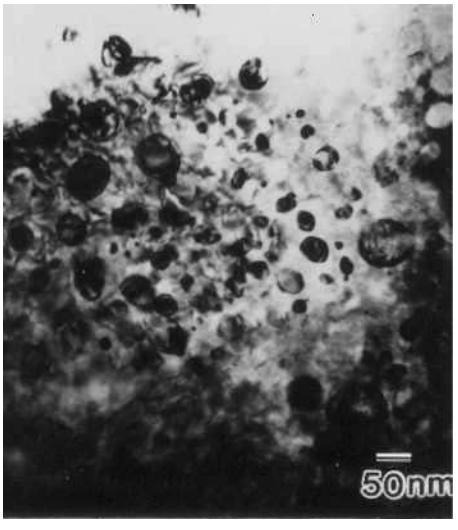

(*a*)

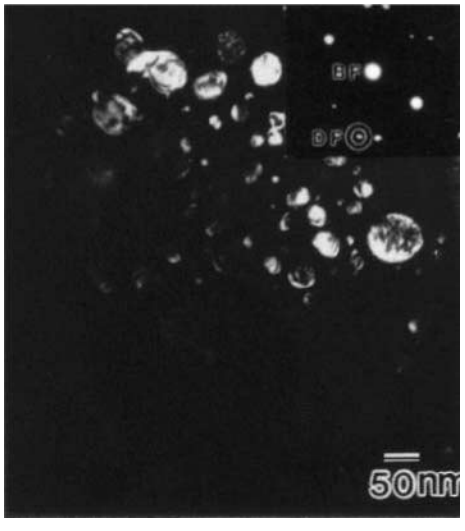

(*b*)

Fig. 6—TEM micrographs showing distribution of the spherical deposits of wire electrode materials in the recast layer, specimen tempered at 600 °C: (*a*) bright field and (*b*) dark field.

As shown in Figure 8, there are many spherical, chromium-rich, sigma phases, with diameters between 120 and 200 nm and within the recast layer. The sigma spheres generally

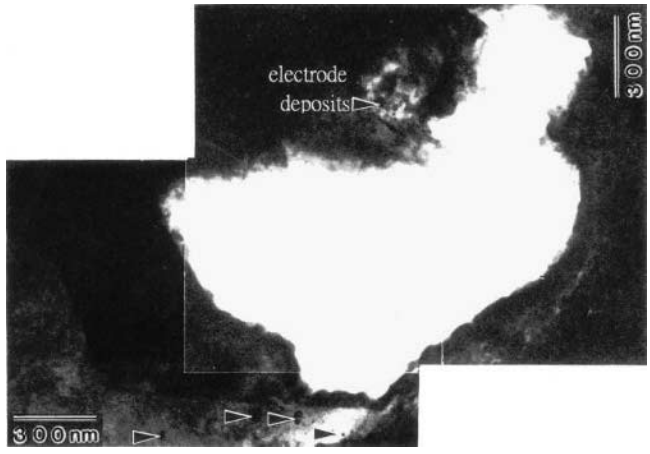

Fig. 7—TEM micrographs showing the structures nearby a gas void induced by WEDM rough cutting.

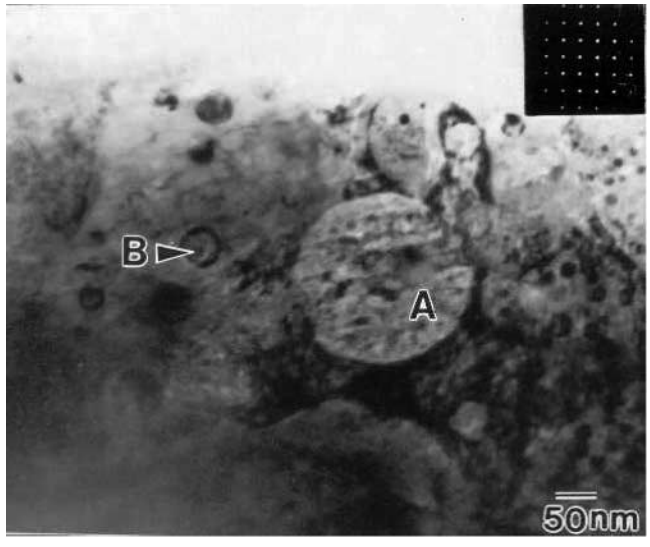

(*a*)

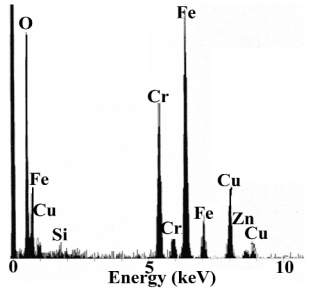

(*b*)

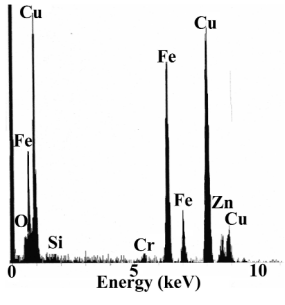

(*c*)

Fig. 8—(*a*) TEM micrographs showing two kinds of spherical deposit or precipitate after WEDM rough cutting: A: larger size Cr-rich sigma sphere, and B: smaller size, electrode material deposit. SAD pattern of sphere A is affixed at the right corner. (*b*) EDX analysis of A in (a) (*c*) EDX analysis of B in (a)

appeared near the bottom of the recast layer, as observed here and in the unpublished work of our group.[14a] This phase does not exist in the tempered martensitic stainless steel before WEDM rough cutting. The sigma sphere contains a very high amount of chromium (*ca*. 44 to 47 wt pct), as detected by the semiquantitative EDX analysis shown in Figure 8(a). It is generally known that sigma phase is usually very difficult to form in the solid state during typical processing thermal cycles. Then, one may question how these sigma spheres are formed. The exclusion of pure solid-state behavior leads us to consider the effect of possible molten-state behavior as well as that of the constituent alloying elements. As seen from the Cr-Fe phase diagram and the melting temperatures of chromium and iron (1863 °C and 1535 °C, respectively), it seems reasonable to predict that chromium preferentially concentrates in the bottom molten region, whereas iron tends to be enriched in the top molten region. Subsequently, suffering from the rapid quenching of the dielectric water, the bottom molten region solidifies with a slower solidification rate while the overheated vapor phase and the top molten region undergo rapid solidification. As the temperature cools down further, sigma phase nucleates within the high-temperature solid solution with a localized concentrated chromium content and continues to grow at a limited rate. Besides, the steel used in this study has a high chromium and molybdenum content, which favor the formation of sigma phase in the solid-state transformation.[14b]

Also present in Figure 8(a) are the numerous electrode deposits with a smaller size of *ca*. 10 to 60 nm. The EDX analysis of one deposit about 50 nm size is shown in Figure 8(c), which indicated the relatively high copper and zinc concentrations of the electrode material.

In the workpiece surface adjacent to the recast layer, a HAZ without temper-induced carbides was detected (Figure 9). The thickness of the HAZ is about 4 μm, based on direct estimation with TEM. According to the microstructure, there are two distinct structures in the HAZ. Adjacent to the recast layer, a lath martensite was observed; next to the lath martensite, a ferrite with an annealed structure and a low dislocation density was found. The reason why these two microstructures were induced in the HAZ can be explained as follows. It is known that austenization of martensitic steel requires the workpiece be heated above 1000 °C to fall within the gamma loop, as seen in Fe-Cr phase diagram.[15] Therefore, when heat is emitted by electrical discharging on the cutting surface, the lath martensite structure was detected directly near the recast layer, due to the phase transformation from austenite to martensite. However, next to the lath martensite, only an annealed structure was found, in which region the temperature increased to below 1000 °C and the structure was not austenized; thus, an annealed ferrite structure with a lower dislocation density was developed. Many researchers[7,16,17] have proved that a white layer of martensitic structure was developed on the surface processed by EDM. However, both fine martensite and annealed structures were observed on the cutting surface in this study. It is worth noting that the temper-induced carbides were almost dissolved in the HAZ. That is, the carbides dissolved in the matrix during heating by electrical discharging but did not reprecipitate, due to rapid cooling from the flushing DI water. Beside the HAZ, a typical tempered martensite with many kinds of carbides was observed (Figures 10 and 11).

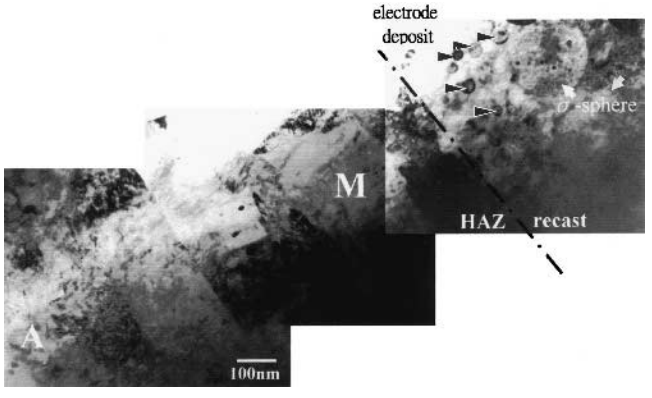

Fig. 9—TEM micrographs showing the interfacial microstructure between recast layer and HAZ after WEDM rough cutting: M: lath martensite; A: annealed structure, and HAZ: heat-affected zone.

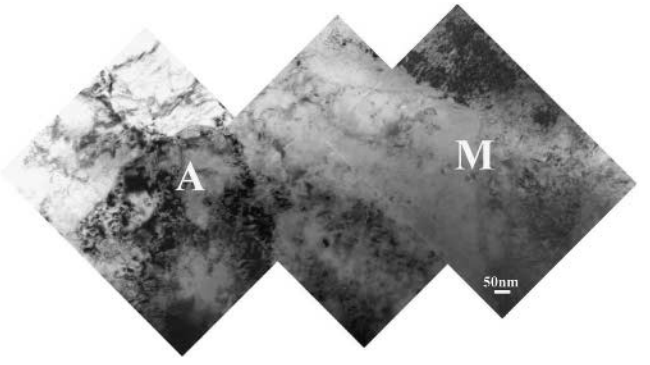

Fig. 10—TEM micrographs showing two distinct microstructures in the HAZ: M: lath martensite; and A: annealed structure.

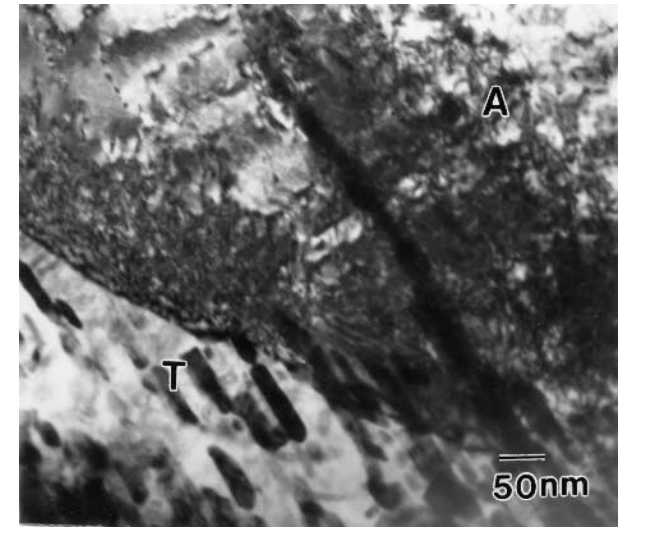

Fig. 11—TEM micrograph showing the tempered martensite adjacent to the annealed structure of HAZ: T: tempered structure, and A: annealed structure.

IV. CONCLUSIONS

Based on the experimental results, the following conclusions are drawn.

1. The thickness of the recast layer formed after WEDM rough cutting is affected by the heat-treatment condition of the martensitic mold steel. The thickness decreases with increasing tempering temperature, and the largest thickness is obtained using quenched mold steel.
2. Surface intergranular cracks were observed on the quenched martensitic steel workpiece after WEDM rough cutting. These surface cracks, caused by relieving of the residual thermal stress of the quenched workpiece, could be avoided with workpieces tempered above 200 °C. The surface cracking initiates and propagates quickly along grain boundaries during rough cutting. All surface cracks were filled with the recast material, which was formed by rapidly melting and/or evaporating the workpiece by electrical discharging and then solidifying it by injection of DI water during WEDM rough cutting.
3. The TEM examination of the 600 °C tempered cross-sectional specimen showed that amorphous and microcrystalline structures could be observed on some parts of the outermost rough cut surface. Also, a porous recast layer, several micrometers thick, was always present on the rough-cut surface. Inside the recast layer, smaller spherical deposits of wire-electrode material, of *ca*. 50 to 60 nm in size, and larger spherical Fe-Cr sigma-phase precipitates, of *ca*. 120 to 200 nm in size, appeared. The sigma precipitates tend to be present near the bottom part of the recast layer. The composition of the sigma sphere was confirmed by EDX analysis, and its formation mechanism was proposed.
4. Adjacent to the recast layer, there is a HAZ about 4-μm thick. Temper-induced carbides were fully dissolved in the zone, and two distinct regions existed: the first region, adjacent to the recast layer, was a lath martensite structure, and the second region was an annealed ferrite structure.

ACKNOWLEDGMENT

The authors thank the National Science Council for the financial support of this research (Grant No. NSC 88-2216-E-182-006).

REFERENCES

1. *ASM Handbook*, 10th ed., vol. 1, *Properties and Selection: Irons, Steels, and High-Performance Alloys*, ASM, Materials Park, OH 1990, pp. 758-79.
2. P. Schwaab *et al*.: *Atlas of Precipitates in Steels*, Verlag Stahleisen mbH, Duesseldorf, 1983, pp. 160-83.
3. W. Koenig: *Fertigungsverfahren Band 3: Abtragen*, VDI Verlag GmbH, Duesseldorf, 1990.
4. P. Beardmore and D. Hull: *J. Inst. Met*., 1966, vol. 94, p. 14.
5. Y. Fukuzawa, Y. Kojima, T. Tani, E. Sekiguti, and N. Mohri: *Mater. Manufacturing Processes*, 1995, vol. 10, p. 195.
6. M.M. Barash and C.S. Kahlon: *Int. J. Mach. Tool Des. Res*., 1964, vol. 4, p. 1.
7. B. Hribernik and F. Russ: *Arch. Eisenhuettenwes*., 1982, vol. 53, p. 373.
8. J.R. Crookall and B.C. Khor: *Proceedings 15th International Machine Tool Design Research Conference,* 1975, p. 373.
9. Y.S. Wong, L.C. Lim, and L.C. Lee: *J. Mater. Processing Technol*., 1995, vol. 48, p. 299.
10. C.A. Huang, H.-J. Klaar, and I.L. Kao: *DGM Metallographie-Tagung*, Rostock, Germany, 1999.
11. H.-J. Klaar and C.A. Huang: *Prakt. Met. Sonderbd.* 1993, vol. 24, p. 333.
12. B.N. Zolotych: *Ueber die Physikalischen Grundlagen der Elektroerosiven Metallbearbeitung. Bd. 1: Elekrtroerosive Bearbeitung von Metallen*, Akademie der Wissenschaften der UdSSR, Moskau, 1957.
13. L.C. Lee, L.C. Lim, Y.S. Wang, and H.H. Lu: *J. Mater. Processing Technol*., 1990, vol. 24, p. 513.
14. P. Duwez and S.C.H. Lin: *J. Appl. Phys*., 1967, vol. 38, p. 4096.

14a. H.H. Kuo: Master's Thesis, 2000, Chang-Gung University, Taiwan, R.O.C.

14b. E.L. Brown: *Metall. Trans. A*, 1983, vol. 14A, pp. 791-800.

15. *ASM Handbook*, 10th ed., vol. 3, *Alloy Phase Diagrams*, ASM, Materials Park, OH, 1992, p. 152.
16. A. Rose and Strassburg: *Arch. Eisenhuetnwes*., 1956, vol. 27, p. 513.
17. W.I. Jutzler: Ph.D. Dissertation, RWTH–Aachen University, Aachen, 1982.